J|A|C|S
ARTICLES
Published on Web 05/11/2004

The Role of Ligand Displacement in Sm(II)−HMPA-Based Reductions

Edamana Prasad,[†] Brian W. Knettle,[‡] and Robert A. Flowers, II*,[†]

Contribution from the Department of Chemistry, Lehigh University, Bethlehem, Pennsylvania 18015, and Department of Chemistry and Biochemistry, Texas Tech University, Box 41061, Lubbock, Texas 79409-1061

Received February 16, 2004; E-mail: rof2@lehigh.edu

Abstract: Addition of HMPA to [Sm{N(SiMe$_3$)$_2$}$_2$] produces a less reactive reductant in contrast to addition of HMPA to SmI_2. While the [Sm{N(SiMe$_3$)$_2$}$_2$]−HMPA combination results in a more powerful reductant based on the redox potential, the observed decrease in reactivity is attributed to steric hindrance caused by the nonlabile ligand −N(SiMe$_3$)$_2$ and HMPA around the Sm metal. The importance of ligand displacement (exchange) in Sm(II)−HMPA-based reactions and insight into the mechanism of [Sm{N(SiMe$_3$)$_2$}$_2$]−HMPA and SmI_2−HMPA reductions are presented.

Introduction

The addition of HMPA to reactions that employ SmI_2 considerably accelerates the electron-transfer process. The seminal work of Inanaga demonstrated that the rate of reduction of organic halides by SmI_2 was increased dramatically upon addition of HMPA.[1] Aside from favorable rate enhancements, HMPA addition to SmI_2 provides increased diastereoselectivities and beneficial product distributions in a wide range of reactions.[2] A study by Molander showed that the addition of HMPA produces a sterically encumbered reductant that not only dictates the diastereoselectivity of reductive coupling reactions, but also stabilizes reactive intermediates (ketyls, radicals) in close proximity to the Sm−HMPA complex, thereby preventing competing reaction processes.[3] Although numerous other additives have been used and alternative protocols have been developed, none appear to approach the general utility of SmI_2−HMPA. Thus, despite its carcinogenicity, HMPA remains the additive of choice for reactions of SmI_2.

Mechanistic studies of Sm(II)-based reagents and the unusual effects of HMPA on them are beginning to appear in the literature. The elegant work of Daasbjerg and Skrydstrup has shown that addition of 4 equiv of HMPA to SmI_2 in THF likely produces [Sm(HMPA)$_4$(THF)$_2$]I$_2$ and addition of greater than 10 equiv of HMPA produces [Sm(HMPA)$_6$]I$_2$.[4] Because HMPA is an excellent donor ligand, displacement of the labile iodide to the outer sphere of the complex is not surprising. Because it is possible to displace I^- upon the addition of HMPA to SmI_2, does this displacement have mechanistic consequences? Limited examination of the reactivity of SmI_2−HMPA and Sm(OTf)$_2$−HMPA shows that these reductant−HMPA combinations have similar reactivity patterns[5] and hence may produce similar intermediates (if $^-$OTf is displaced in a manner analogous to I^-). Conversely, hard, basic alkoxide and amide ligands should have a higher affinity for Sm(II) and as a result would be less likely to be displaced upon addition of HMPA or basic substrates. Upon addition of HMPA to SmI_2, the reducing power of the complex is enhanced,[4,6] and the rates of reaction increase dramatically; that is, enhanced reducing power leads to faster reaction rates.[1,7] Based on the brief discussion above, one may ask, how does HMPA influence the reducing power and rates of reduction for a Sm(II) reductant containing a less labile ligand? Is ligand displacement mechanistically important in the reduction of various organic functional groups? To initially address these questions, the impact of HMPA on the redox potential and rates of reaction of a Sm(II) complex containing the less labile −N(SiMe$_3$)$_2$ ligand was examined. The experiments presented herein show that ligand displacement upon HMPA addition plays a role in the reduction of organic functional groups by Sm(II) reagents, presumably through altering the steric environment of the reductant.

Experimental Section

Material and General Procedures. THF was distilled from sodium benzophenone ketyl, under nitrogen atmosphere. HMPA was dried by vacuum distillation from calcium oxide and degassed and backfilled with N_2 at least three times to remove all oxygen. Dried solvents were stored in an Innovative Technology, Inc. drybox containing a nitrogen atmosphere and a platinum catalyst for drying. The [Sm{N(SiMe$_3$)$_2$}$_2$] complex was prepared according to the procedure of Evans.[8] The

[†] Lehigh University.
[‡] Texas Tech University.

(1) Inanaga, J.; Ishikawa, M.; Yamaguchi, M. *Chem. Lett.* **1987**, 1485.
(2) (a) Molander, G. A. *Chem Rev.* **1992**, *92*, 29. (b) Molander, G. A.; Harris, C. R. *Chem. Rev.* **1996**, *96*, 307. (c) Steel, P. G. *J. Chem. Soc., Perkin Trans. 1* **2001**, 2727.
(3) Molander, G. A.; McKie, J. A. *J. Org. Chem.* **1992**, *57*, 3132.
(4) Enemaerke, R. J.; Hertz, T.; Skrydstrup, T.; Daasbjerg, K. *Chem.-Eur. J.* **2000**, *6*, 3747.
(5) Fukuzawa, S.; Mutoh, K.; Tsuchimoto, T.; Hiyama, T. *J. Org. Chem.* **1996**, *61*, 5400.
(6) (a) Shabangi, M.; Flowers, R. A., II. *Tetrahedron Lett.* **1997**, *38*, 1137. (b) Shabangi, M.; Kuhlman, M. L.; Flowers, R. A., II. *Org. Lett.* **1999**, *1*, 2133. (c) Enemaerke, R. J.; Daasbjerg, K.; Skrydstrup, T. *Chem. Commun.* **1999**, 343−344.
(7) Prasad, E.; Flowers, R. A., II. *J. Am. Chem. Soc.* **2002**, *124*, 6895.

concentration of the Sm complex was determined by iodometric titration.[9] 2-Butanone and 1-iodobutane were purchased from Aldrich and distilled under vacuum from calcium oxide before use.

The redox potential of the [Sm{N(SiMe$_3$)$_2$}$_2$]−HMPA complex was measured by cyclic voltammetry, employing a BAS 100B/W MF-9063 Electrochemical Workstation. The working electrode was a standard glassy carbon electrode. The electrode was polished with polishing alumina and cleansed in an ultrasonic bath. The auxiliary electrode was a platinum wire, and the reference electrode was a saturated Ag/AgNO$_3$ electrode. The scan rate for all experiments was 100 mV/s. The electrolyte used was tetrabutylammonium hexafluorophosphate. The concentration of the Sm(II) species in each experiment was 0.50 mM. All solutions were prepared in the drybox and transferred to the electrochemical analyzer for analysis.

UV−vis experiments were performed on a Shimadzu UV-1601 UV-visible spectrophotometer controlled by UV Probe (version 1.11) software. The VPO experiments were carried out on a Wescor 5500-XR vapor pressure osmometer operating at 25 °C in a drybox. Calibration curves of VPO reading versus molality were obtained using biphenyl as the calibration standard.[9]

Stopped-Flow Studies. Kinetic experiments in THF were performed with a computer-controlled SX-18 MV stopped-flow reaction spectrophotometer (Applied Photophysics Ltd. Surrey, UK). The [Sm{N(SiMe$_3$)$_2$}$_2$]−HMPA complex and substrates were taken separately in airtight Hamilton syringes from a drybox and injected into the stopped-flow system. The cell box and the drive syringes of the stopped-flow reaction analyzer were flushed a minimum of three times with dry, degassed solvents to make the system oxygen-free. The concentration of [Sm{N(SiMe$_3$)$_2$}$_2$]−HMPA complexes used for the study was 20 mM. The concentration of the substrates was kept high relative to [Sm{N(SiMe$_3$)$_2$}$_2$]−HMPA (0.20−0.40 M) to maintain pseudo-first-order conditions. The reaction rate constants were determined using standard methods.[10] Reaction rates were determined from the decays of the [Sm{N(SiMe$_3$)$_2$}$_2$]−HMPA complex at 555 nm. The decay of the [Sm{N(SiMe$_3$)$_2$}$_2$] or the HMPA complex displayed first-order behavior over >4 half-lives for [Sm{N(SiMe$_3$)$_2$}$_2$]−substrate combinations. The kinetics for 2-butanone followed the rate law (1) shown below.

$$-\mathrm{d[Sm(II)\ complex]}/\mathrm{d}t = k\mathrm{[Sm(II)\ complex][ketone]} \quad (1)$$

The kinetics of 1-iodobutane followed the rate law (2) shown below.

$$-\mathrm{d[Sm(II)\ complex]}/\mathrm{d}t = 2k\mathrm{[Sm(II)\ complex][alkyl\ iodide]} \quad (2)$$

A representative stopped-flow trace for the reduction of 2-butanone by [Sm{N(SiMe$_3$)$_2$}$_2$]−HMPA (10 equiv) is shown in Figure 1. The temperature studies used to determine activation parameters were carried out over a range of 30−50 °C using a Neslab circulator connected to the sample-handling unit of the stopped-flow system. The step size used for the temperature study was 5 °C, and each kinetic trace was recorded at a known temperature that was monitored by a thermocouple in the reaction cell. The temperature measurements are accurate to 0.01 °C.

Results and Discussion

Because HMPA is a hazardous material, one of the goals of numerous research programs is the design of protocols that mimic the favorable features of SmI$_2$−HMPA, but do not require the presence of the carcinogenic additive. A detailed mechanistic understanding of the role of HMPA in reactions of SmI$_2$ and other Sm-based reductants will provide the insight necessary to design alternative protocols for mimicking the useful features of SmI$_2$−HMPA. The goal of this work was to establish the importance of HMPA-induced ligand displacement in reactions of Sm(II)-based reductants. Experiments described herein were designed to examine the effect of HMPA addition on a Sm reductant containing a nonlabile ligand. Beginning experiments were initiated to establish the effect of HMPA on the reducing power of the [Sm{N(SiMe$_3$)$_2$}$_2$] complex in THF. Follow-up experiments established the likely structure of the complex formed between [Sm{N(SiMe$_3$)$_2$}$_2$] and HMPA and examined the rates for reduction of 1-iodobutane and 2-butanone. With these data, comparisons of both structure and reactivity could be made for the [Sm{N(SiMe$_3$)$_2$}$_2$]−HMPA complex and the one formed between SmI$_2$ and HMPA.

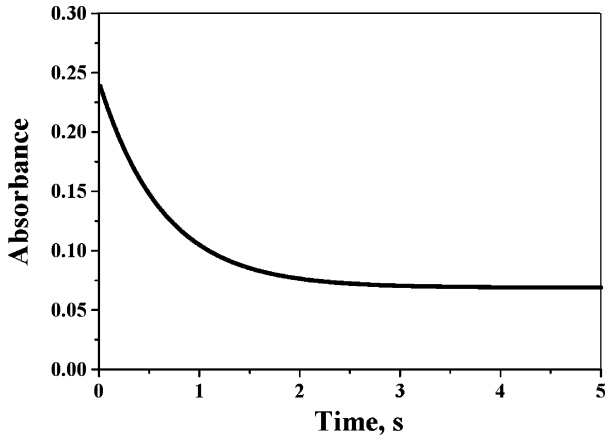

Figure 1. Stopped-flow decay trace of Sm{N[Si(CH$_3$)$_3$]$_2$}$_2$ (0.02 M) in the presence of 2-butanone (0.20 M) and HMPA (10 equiv to Sm(II) complex concentration) in THF.

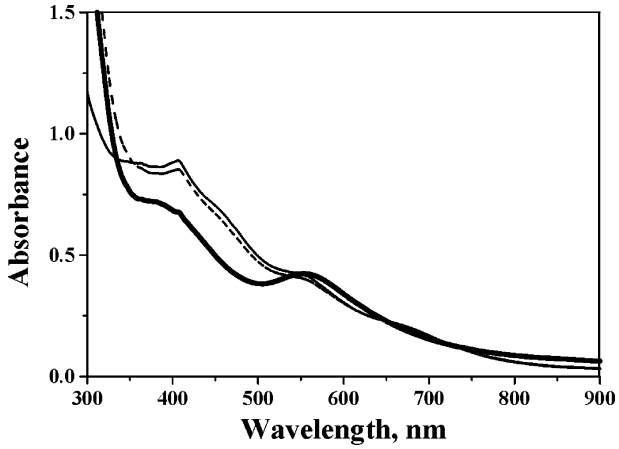

Figure 2. The UV−vis spectra of [Sm{N(SiMe$_3$)$_2$}$_2$] (thick solid line) and [Sm{N(SiMe$_3$)$_2$}$_2$] containing 2 and 10 equiv of HMPA in THF (dashed and thin solid lines, respectively).

Figure 2 shows the UV−vis spectrum for [Sm{N(SiMe$_3$)$_2$}$_2$] and the spectra after the addition of 1 and 10 equiv of HMPA. Upon addition of 1 equiv of HMPA, there is a slight blue shift of the absorbance at 555 nm. A broad shoulder begins to appear at 670 nm. Also, the intensity of the broad absorption at 410 nm sharpens to some extent. Further addition of HMPA (up to 10 equiv) displayed no further change in the UV−vis spectrum. The absorption bands in Sm(II) complexes have been attributed to f to d ($4f^n$ to $4f^{n-1}5d^1$) transitions.[11] Because the d orbitals are spatially extended towards the ligand field, it is reasonable

(8) Evans, W. J.; Drummond, D. K.; Zhang, H.; Atwood, J. L. *Inorg. Chem.* **1988**, *27*, 575.
(9) Shotwell, J. B.; Sealy, J. M.; Flowers, R. A., II. *J. Org. Chem.* **1999**, *64*, 5251.
(10) Pedersen, S. U.; Lund, T.; Daasbjerg, K.; Pop, M.; Fussing, I.; Lund, H. *Acta Chem. Scand.* **1998**, *52*, 657.

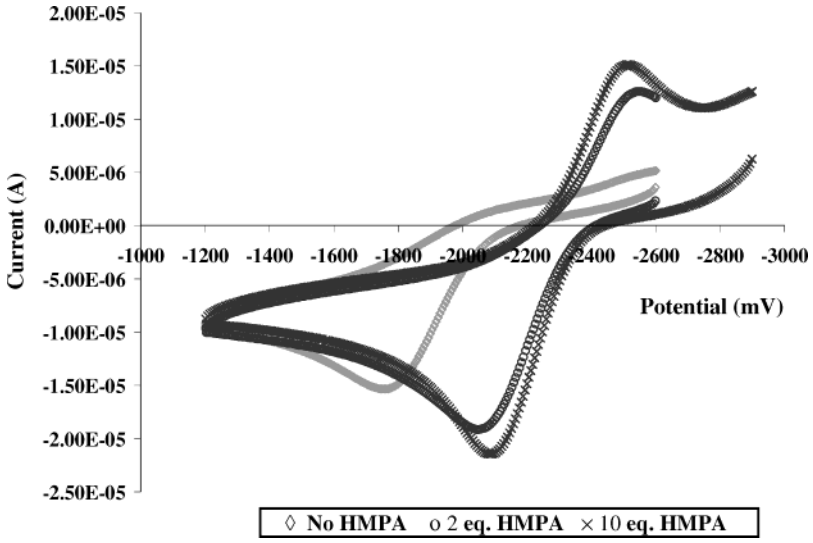

Figure 3. Cyclic voltammogram of $[Sm\{N(SiMe_3)_2\}_2]$ and $[Sm\{N(SiMe_3)_2\}_2]$ containing 2 and 10 equiv of HMPA at a glassy carbon electrode in THF versus $Ag/AgNO_3$ (sat'd) reference electrode.

to assume that displacement of THF by HMPA would result in a perturbation of d orbital energy and hence a change in the UV−vis spectrum. Upon addition of HMPA to SmI_2, there is a pronounced blue shift in the UV−vis spectrum.[4a,9] Addition of HMPA to $[Sm\{N(SiMe_3)_2\}_2]$ also exhibits similar (although less pronounced) changes in the UV−vis spectrum. Regardless of the exact nature of the electronic transitions, comparison of the absorption data with that obtained for SmI_2−HMPA clearly shows that the complex obtained by addition of HMPA to $[Sm\{N(SiMe_3)_2\}_2]$ is unique.

Next, cyclic voltammetry was utilized to estimate the thermodynamic redox potential of $[Sm\{N(SiMe_3)_2\}_2]$ in THF and the impact of HMPA on the reducing power of the complex. The voltammogram of $[Sm\{N(SiMe_3)_2\}_2]$ was irreversible (Figure 3), and the redox potential was found to be -2.1 ± 0.1 V (vs sat'd $Ag/AgNO_3$).[12] Addition of 2 equiv of HMPA to the complex produced a reductant with a redox potential of -2.5 ± 0.1 V. Addition of up to 10 equiv of HMPA showed no further impact on the redox potential. Another notable feature of these experiments was that, upon addition of HMPA, the irreversible voltammogram became quasireversible. The cyclic voltammetry experiment clearly shows that a more powerful reductant (in thermodynamic terms) is produced upon addition of HMPA to $[Sm\{N(SiMe_3)_2\}_2]$ in a manner analogous to SmI_2.

The experiments described to this point indicate that addition of HMPA to $[Sm\{N(SiMe_3)_2\}_2]$ produces a reductant that is unique as compared to the complex formed upon the addition of HMPA to SmI_2. However, these studies do not address the solution structure of the active reductant in solution. Examination of the $[Sm\{N(SiMe_3)_2\}_2(THF)_2]$ complex prepared by Evans and co-workers shows that it is highly unlikely that more than 1 or 2 equiv of HMPA can be accommodated.[8] To examine this issue in more detail, vapor pressure osmometry (VPO) was utilized to gain insight into the structure (MW) of the active reductant in solution. Addition of 1 equiv of HMPA to a standardized solution of $[Sm\{N(SiMe_3)_2\}_2]$ in THF provided a MW corresponding to $[Sm\{N(SiMe_3)_2\}_2(HMPA)]$. Addition of 2 equiv of HMPA provided data consistent with the average of the MW of $[Sm\{N(SiMe_3)_2\}_2(HMPA)]$ and HMPA. Calorimetric experiments were performed to estimate the stoichiometry of the complex by titration of excess HMPA into a solution of $[Sm\{N(SiMe_3)_2\}_2]$ in THF.[9] Although it was difficult to obtain statistically stable fits of the data, repeated experiments provided results consistent with coordination of 2 equiv of HMPA (Supporting Information). If a second equivalent of HMPA is coordinating to $[Sm\{N(SiMe_3)_2\}_2(HMPA)]$, it is likely to have a lower affinity than the first ligand, presumably due to steric crowding around Sm. In the absence of definitive crystallographic data, the collective evidence is consistent with $[Sm\{N(SiMe_3)_2\}_2(HMPA)_2]$ as the active reductant formed between $[Sm\{N(SiMe_3)_2\}_2]$ and 10 equiv of HMPA.

Although the VPO and calorimetric data do not clearly discern whether 1 or 2 equiv of HMPA is coordinated to the Sm−silylamide complex, the electrochemical data show that a more powerful reductant is formed upon addition of HMPA to $[Sm\{N(SiMe_3)_2\}_2]$. Because the hallmark of the SmI_2−HMPA combination is enhanced rates of reduction of a wide range of functional groups (as compared to SmI_2), a series of stopped-flow experiments were carried out to examine the impact of HMPA on the rates of reduction of 1-iodobutane and 2-butanone by $[Sm\{N(SiMe_3)_2\}_2]$. Reduction of 1-iodobutane produced butane, while reduction of 2-butanone produced the pinacol product after workup. Figure 4 shows a plot of *k* versus HMPA concentration for the reduction of 1-iodobutane by $[Sm\{N(SiMe_3)_2\}_2]$. The experiment yielded interesting results. Upon the addition of 1 equiv of HMPA, the rate of reduction of 1-iodobutane was enhanced. However, upon further addition of another equivalent of HMPA, the rate of reduction decreased. Further addition of 6 and then 10 equiv of HMPA to $[Sm\{N(SiMe_3)_2\}_2]$ showed that the rate decreased and leveled out at 10 equiv. Subsequent addition of up to 25 equiv of HMPA provided no further decrease in the rate. The same experiment was carried out using 2-butanone as the substrate and yielded similar results (see Supporting Information). The rate data described in Figure 4 show that an excess of HMPA is required to bring the rate of reduction of 1-iodobutane to a steady value. It is likely that addition of 1 equiv of HMPA to $[Sm\{N(SiMe_3)_2\}_2]$

(11) Dorenbos, P. *J. Phys.: Condens. Matter* **2003**, *15*, 575.
(12) Prasad, E.; Knettle, B. W.; Flowers, R. A., II. *J. Am. Chem. Soc.* **2002**, *124*, 14663.

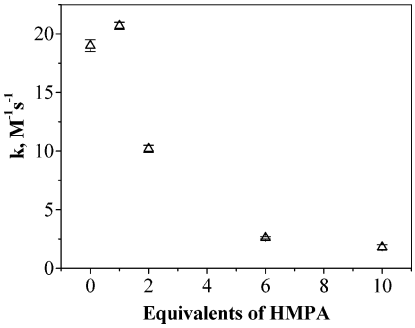

Figure 4. A plot of k versus equivalents of HMPA in $Sm\{N[Si(CH_3)_3]_2\}_2$/1-iodobutane in THF.

Table 1. Rate Constants and Activation Parameters for the Reduction of 2-Butanone and 1-Iodobutane by $[Sm\{N(SiMe_3)_2\}_2]$ and $[Sm\{N(SiMe_3)_2\}_2]$ Containing 10 equiv of HMPA

system	k^{b-d} $M^{-1}\,s^{-1}$	$\Delta S^{\ddagger,e}$ cal $mol^{-1}\,K^{-1}$	$\Delta H^{\ddagger,e}$ kcal mol^{-1}	$\Delta G^{\ddagger,f}$ kcal mol^{-1}
$[Sm\{N(SiMe_3)_2\}_2]$− 2-butanone[a]	$(1.7 \pm 0.3) \times 10^2$	-43 ± 1	1.4 ± 0.3	14.8 ± 0.6
$[Sm\{N(SiMe_3)_2\}_2]$− 2-butanone− 10 equiv of HMPA	16 ± 1	-17 ± 1	11.6 ± 0.4	17.0 ± 0.5
$[Sm\{N(SiMe_3)_2\}_2]$− 1-iodobutane[a]	19 ± 1	-47 ± 1	1.7 ± 0.1	16.5 ± 0.3
$[Sm\{N(SiMe_3)_2\}_2]$− 1-iodobutane− 10 equiv of HMPA	1.8 ± 0.2	-20 ± 1	11 ± 1	17 ± 1

[a] Data initially reported in ref 7. [b] All rate data are the average of at least two independent runs. [c] Experimental uncertainties were propagated through these calculations, and all values are reported as $\pm\sigma$. [d] All rate studies were carried out at 25 °C. [e] Eyring activation parameters were obtained from $\ln(k_{obs}h/kT) = -\Delta H^{\ddagger}/RT + \Delta S^{\ddagger}/R$. [f] Calculated from $\Delta G^{\ddagger} = \Delta H^{\ddagger} - T\Delta S^{\ddagger}$.

produces a more powerful reductant still capable of interacting with substrate while the decrease in rate of reduction of 1-iodobutane and 2-butanone upon further addition of HMPA is presumably due to a higher degree of shielding of the Sm by the bulky HMPA and $-N(SiMe_3)_2$ ligands.

To obtain more information on this behavior, the activation parameters for the reduction of both substrates by $[Sm\{N(SiMe_3)_2\}_2]$ containing 10 equiv of HMPA were determined. The results and comparison to reduction by $[Sm\{N(SiMe_3)_2\}_2]$ alone[12] are given in Table 1.

Examination of the rate constants shows that, in the reduction of either 2-butanone or 1-iodobutane, the presence of HMPA significantly decreases the rate of reduction of both substrates by an order of magnitude even though $[Sm\{N(SiMe_3)_2\}_2]$−HMPA is a more powerful reductant (based on its thermodynamic redox potential). The activation parameters are consistent with less order and a higher degree of bond reorganization in the activated complex in the presence of HMPA, findings distinctly different for those determined for reduction of ketones and alkyl iodides by $[Sm(THF)_2(HMPA)_4]I_2$ and $[Sm(HMPA)_6]I_2$. For instance, reduction of 2-butanone and 1-iodobutane by SmI_2 was faster upon the addition of HMPA, and the presence of the sterically demanding ligand leads to negative entropies of activation in the range of -40 cal $mol^{-1}\,K^{-1}$ with relatively low enthalpies of activation. These studies were interpreted to be consistent with coordination between substrates and SmI_2−HMPA, presumably occurring through displacement of a ligand by substrate. Conversely, the more positive entropies of activation and higher enthalpies of activation obtained upon the addition of HMPA to $[Sm\{N(SiMe_3)_2\}_2]$ indicate that addition of HMPA to $[Sm\{N(SiMe_3)_2\}_2]$ provides a reductant incapable of interaction with substrates through inner-sphere interactions with the metal center. Taken together, these results suggest that addition of HMPA to SmI_2 results in a reductant which provides open coordination sites for substrate along the reaction coordinate and addition of HMPA to $[Sm\{N(SiMe_3)_2\}_2]$ which contains a nonlabile ligand leads to a less reactive reductant.

The evidence described above suggests that providing a more powerful reductant through HMPA addition is not sufficient to produce a more reactive species. Substrate access to the metal center is of paramount importance as well. The role of ligand displacement and the interplay between substrate access and reducing power of Sm(II) complexes has not been addressed in previous studies, but reasonable inferences can be drawn from comparison to related systems. Recently, Hilmersson and coworkers have developed a cosolvent mixture capable of accelerating reactions of SmI_2 utilizing addition of water and amines.[13] This combination of reagents significantly accelerates the rate of reduction of numerous functional groups and in some cases reduces substrates more efficiently than SmI_2−HMPA. Although extensive mechanistic studies have not been carried out on the SmI_2/H_2O/amine reducing system, there are two important features of this combination worth mentioning. First, it is believed that displacement of iodide through precipitation of ammonium iodide provides the driving force for the reaction. Second, the redox potential of the SmI_2/H_2O/amine system in THF is nearly identical to that of SmI_2 alone.[14] Thus, coordination of a strong electron donor ligand such as HMPA and production of a more powerful ground-state reductant is not a precondition for accelerating reactions of SmI_2.

Conclusions

The high reactivity of SmI_2−HMPA toward ketones and alkyl iodides is a consequence of HMPA-induced iodide displacement which provides open coordination sites for substrate access to the Sm reductant. Replacement of iodide with the less labile $-N(SiMe_3)_2$ leads to a less reactive reagent upon addition of HMPA through the creation of a sterically encumbered reductant incapable of providing substrate access through ligand exchange. Although addition of HMPA to SmI_2 or $[Sm\{N(SiMe_3)_2\}_2]$ provides a thermodynamically more powerful reductant, enhanced reducing power of the ground-state reductant is not a requirement for increased reactivity. This facet of Sm(II)−HMPA chemistry should be considered in the design of new approaches to enhance the reactivity of Sm(II)-based reductants.

Acknowledgment. R.A.F. is grateful to the National Science Foundation (CHE-0413845) for support of this work. We also thank Drs. Rebecca S. Miller and Sudhadevi Paivallickal for their useful comments on the manuscript.

Supporting Information Available: General experimental details, decay traces, and plots of rate data. This material is available free of charge via the Internet at http://pubs.acs.org.

JA049161J

(13) (a) Dahlen, A.; Hilmersson, G. *Tetrahedron Lett.* **2002**, *43*, 7197. (b) Dahlen, A.; Hilmersson, G. *Chem.-Eur. J.* **2003**, *9*, 1123. (c) Dahlen, A.; Hilmersson, G. *Tetrahedron Lett.* **2003**, *44*, 2661. (d) Dahlen, A.; Petersson, A.; Hilmersson, G. *Org. Biomol. Chem.* **2003**, *1*, 2423. (e) Dahlen, A.; Sundgren, A.; Lahmann, M.; Oscarson, S.; Hilmersson, G. *Org. Lett.* **2003**, *5*, 4085. (f) Kim, M.; Knettle, B. W.; Dahlen, A.; Hilmersson, G.; Flowers, R. A., II. *Tetrahedron* **2003**, *59*, 10397.

(14) Dahlen, A.; Hilmersson, G.; Knettle, B. W.; Flowers, R. A., II. *J. Org. Chem.* **2003**, *68*, 4870.